STRUCTURE AND REACTIVITY OF RUTHENIUM(III) ANTICANCER COMPLEXES

3.1 Introduction

As discussed in chapter 1, ruthenium complexes could be an alternative to the use of the classic platinum anticancer drugs.[1,2] An example of this type of complexes is NAMI-A which shows a remarkable activity against the cancer metastases formation[3] and recently completed phase II clinical trials.[4,5] The interaction mechanism of ruthenium(III) complexes and their ultimate target, DNA or protein has been the subject of extensive research over the last 25 years. Two mechanisms *i.e.* activation by reduction[6,7] and activation by hydrolysis[8,9] have recently been proposed for ruthenium(III) complexes towards biomolecular targets. Activation by reduction is based on the assumption that ruthenium(III) complexes are likely to remain in the inactive state until they reach the tumor site and after reaching the tumor environment, reduction to more active ruthenium(II) occurs due to the lower oxygen content and higher acidity than that of normal tissue.[10,11] Whereas, in activation by hydrolysis, ruthenium(III) complexes are subjected to hydrolysis after dissolution by the ligand exchange process.[12] These results provide a better insight into the interaction mechanism of ruthenium(II/III) complexes with biomolecular targets. In case of NAMI-A, very interesting information has been reported examining the crystal structure of adduct between lactoferrin—NAMI-A and carbonic anhydrase—NAMI-A.[13,14] The crystal structure of carbonic anhydrase—NAMI-A adduct reveals that ligands of ruthenium complex are progressively lost during protein binding and in final adduct ruthenium is found to be associated with amino acid residues such as imidazolium nitrogen atom of His64 and carbonyl oxygen atom of Asn62.[14] Recently, Mazuryk *et al*. has investigated the binding properties of NAMI-A with apo-transferrin.[15] They have reported that NAMI-A and its reduced form binds with the apo-transferrin by formation of aqua derivatives and the presence of at least one labile aqua ligand is sufficient to form adducts. Some *in vivo* and *in vitro* studies have shown that albumin—NAMI-A adduct substantially reduces the biological activity of human carcinoma cells and mammary carcinoma cells in comparison to NAMI-A alone.[16] Again, treatment of human colorectal cancer with (IndH)[trans-$RuCl_4(Ind)_2$] — apo-Tf adduct exhibits high antiproliferative activity in relation to free complex.

Thus, it is believed that these proteins successfully deliver ruthenium complexes into the tumor cells.[17] These results motivated us to study the interaction of ruthenium complexes with albumin to obtain a better insight in to their mechanism of interaction inside the receptor.

In the past two decades, scientists were using computational methods to analyze the molecular properties and the mode of action of different drugs. Conceptual DFT provides a series of reactivity descriptors (global hardness[18], chemical potential, softness[19], electronegativity, etc.) for the description of a chemical processes. QSAR model is widely used to describe toxicity of drug molecules from their chemical structures and corresponding physicochemical properties. In some recent QSAR studies DFT based reactivity parameters have been used successfully to obtain the most accurate QSAR model.[20,21] Chattaraj *et al*.[22] has recently reviewed the importance of DFT based reactivity descriptors for the development of QSAR model. Electrophilicity has been used effectively in developing QSAR model to describe toxicity and biological activity of different organic molecule.[23,24]

In this study, quantum chemical calculations have been performed to investigate the structure and reactivity of ruthenium(III) complexes, such as imidazolium [*trans*-$RuCl_4$ (3H-imidazole) (DMSO-S)] (**I**), indazolium [*trans*-$RuCl_4$ (2H-indazole) (DMSO-S)] (**II**), 1,3,4-triazolium [*trans*-$RuCl_4$ (4H-1,3,4-triazole) (DMSO-S)] (**III**), 4-amino-1,2,4-triazolium [*trans*-$RuCl_4$ (4-amino-1,2,4-triazole) (DMSO-S)] (**IV**), 4-methyl-1,3,4-triazolium [*trans*-$RuCl_4$ (4-methyl-1,3,4-triazole) (DMSO-S)] (**V**) and imidazolium [*trans*-$RuCl_4$(3H-imidazole)$_2$] (**VI**). To study the activity of these ruthenium complexes, we have evaluated global reactivity descriptors such as global hardness, electrophilicity and chemical potential and local philicity which is a local reactivity descriptor. Variation of reactivity trend on inclusion of solvent effect has also been demonstrated. Simple linear regression technique is carried out to build a QSAR model by using calculated reactivity descriptors in order to investigate the cytotoxic activity of the ruthenium complexes against HT-29 colon carcinoma cell line in both gas and solvent phases.

3.2 Computational details

GAUSSIAN 09 program package[30] is employed to carry out DFT calculations at Becke's[31] three parameter hybrid exchange functional (B3) and the Lee-Yang-Parr correlation functional (LYP) (B3LYP)[32] to study electronic structure and properties of ruthenium metal complexes. LANL2DZ basis set,[33] which describe effective core potential of Wadt and Hay (Los Alamos ECP) on ruthenium atom and 6-31G (d, p) basis set[34] for all other atoms are used for ground state geometry optimization. The gas and solvent phase optimization of the ruthenium complexes have been done using unrestricted B3LYP method without imposing any symmetry constrain with tight convergence criteria. A vibrational analysis has been performed to ensure achieving true minimum. To incorporate the solvent effect (water) on the minimum energy structure, a solvation method of polarizable continuum model (PCM)[35] using the integral equation formalism (IEF) variant are considered in this study. Various global reactivity descriptors such as global hardness (η), chemical potential (μ), electrophilicity (ω) and local reactivity descriptor namely local philicity (ω^{+}) have been calculated using respective standard equations described in the theoretical background section. One parameter QSAR studies[36] have been performed using the least square error estimation method[37] to evaluate and compare the cytotoxicity (log IC_{50}^{-1}) of ruthenium complexes.

3.3 Results and discussion

3.3.1 Structure

The significant geometrical parameters of optimized complexes evaluated in the gas and the solvent phases are listed in Table 3.1 and their gas phase optimized geometry evaluated by DFT at B3LYP level are shown in Fig.3.1. The complex **I** containing ruthenium(III) as a central atom shows distorted octahedral configuration with four equatorial chloride ligands and two axial ligands namely DMSO and imidazole molecules. The Ru—Cl1, Ru—Cl2, Ru—Cl3, Ru—Cl4, Ru—N1 and Ru—S1 bond distances in gas phase are found to be 2.393, 2.430, 2.474, 2.443, 2.099 and 2.405 Å, respectively. The bond angles Cl1—Ru—Cl2, Cl2—Ru—Cl3, Cl3—Ru—Cl4 and Cl4—Ru—Cl1 are calculated to be 90.4, 90.2, 88.4 and 90.9^{0}, respectively. However, the bond angle N1—Ru—S1 (178.1^{0}) reflects a little deviation from its experimental

value (176.9^0). Similar geometrical parameters are reported by Zheng and his coworker on studying the aquation of NAMI-A.[38] A slight variation of the bond angles have been noticed when the solvent effect is taken into consideration (Table 3.1). We obtained a distorted octahedral structure of complex **II** and geometrical parameters of the complex are found to be comparable with the experimental data of complex **IV**. In case of complex **III**, we got a pseudo octahedral configuration where 1, 3, 4-triazole ligand coordinates via the N1 atom to ruthenium(III) in the axial position.[39] The Ru—Cl2 bond length is found to be longer while Ru—Cl1, Ru—Cl3, Ru—Cl4, Ru—N1 and Ru—S1 bond lengths are shorter than that of complex **I** in their gas phase. Our calculated geometries of complexes **IV** and **V** are closer to their reported X-ray data.[40] It is noticed from Table 3.1 that the geometry of complex **VI** is comparable with geometry of complex **I**. This complex adopts a pseudo octahedral configuration with two imidazole ligand in their axial positions. Thus it is observed that the computed structural parameters of studied complexes are comparable to the X-ray crystallographic data. However, slightly higher values of bond lengths observed for all complexes from the experimental data can be thought as systematic errors caused by computation method, basis set and environment factors.[38]

Table 3.1 Selected bond lengths (Å) and bond angles (^{0}) calculated for all complexes at B3LYP level both in the gas phase and solvent phase. Solvent phase calculated values are given in parenthesis.

Parameters	**I**	**I** (X- ray)	**II**	**III**	**IV**	**IV** (X-ray)	**V**	**V** (X-ray)	**VI**
Ru—Cl1	2.393 (2.427)	2.345	2.384 (2.422)	2.391 (2.423)	2.373 (2.421	2.357	2.391 (2.426)	2.337	2.442 (2.444)
Ru—Cl2	2.430 (2.433)	2.323	2.421 (2.425)	2.442 (2.432)	2.466 (2.439)	2.341	2.442 (2.432)	2.342	2.442 (2.442)
Ru—Cl3	2.474 (2.439)	2.359	2.451 (2.431)	2.473 (2.439)	2.495 (2.442)	2.354	2.473 (2.437)	2.362	2.442 (2.444)
Ru—Cl4	2.443 (2.434)	2.340	2.484 (2.455)	2.428 (2.432)	2.411 (2.429)	2.373	2.429 (2.431)	2.381	2.442 (2.441)
Ru—N1	2.099 (2.107)	2.081	2.118 (2.129)	2.097 (2.111)	2.099 (2.109)	2.091	2.097 (2.109)	2.094	2.101 (2.123)
Ru—S1	2.405 (2.439)	2.296	2.398 (2.423)	2.396 (2.423)	2.405 (2.437)	2.291	2.398 (2.427)	2.278	-
N1—Ru—S1	178.1 (178.6)	176.9	178.5 (178.9)	178.1 (178.9)	176.9 (177.9)	177.4	178.1 (178.7)	179.1	-
Cl1—Ru—Cl2	90.4 (89.5)	90.8	91.3 (89.9)	90.9 (89.8)	90.3 (89.2)	-	90.9 (89.9)	-	88.7 (89.6)
Cl2—Ru—Cl3	90.2 (90.8)	89.3	90.6 (91.0)	88.4 (90.1)	87.2 (89.4)	-	88.4 (90.3)	-	91.3 (90.4)
Cl3—Ru—Cl4	88.4 (90.0)	89.7	88.6 (90.1)	90.1 (90.6)	89.8 (90.6)	-	90.1 (90.4)	-	88.7 (89.6)
Cl4—Ru—Cl1	90.9 (89.6)	90.2	89.5 (88.9)	90.4 (89.4)	92.6 (90.7)	-	90.4 (89.4)	-	91.3 (90.4)

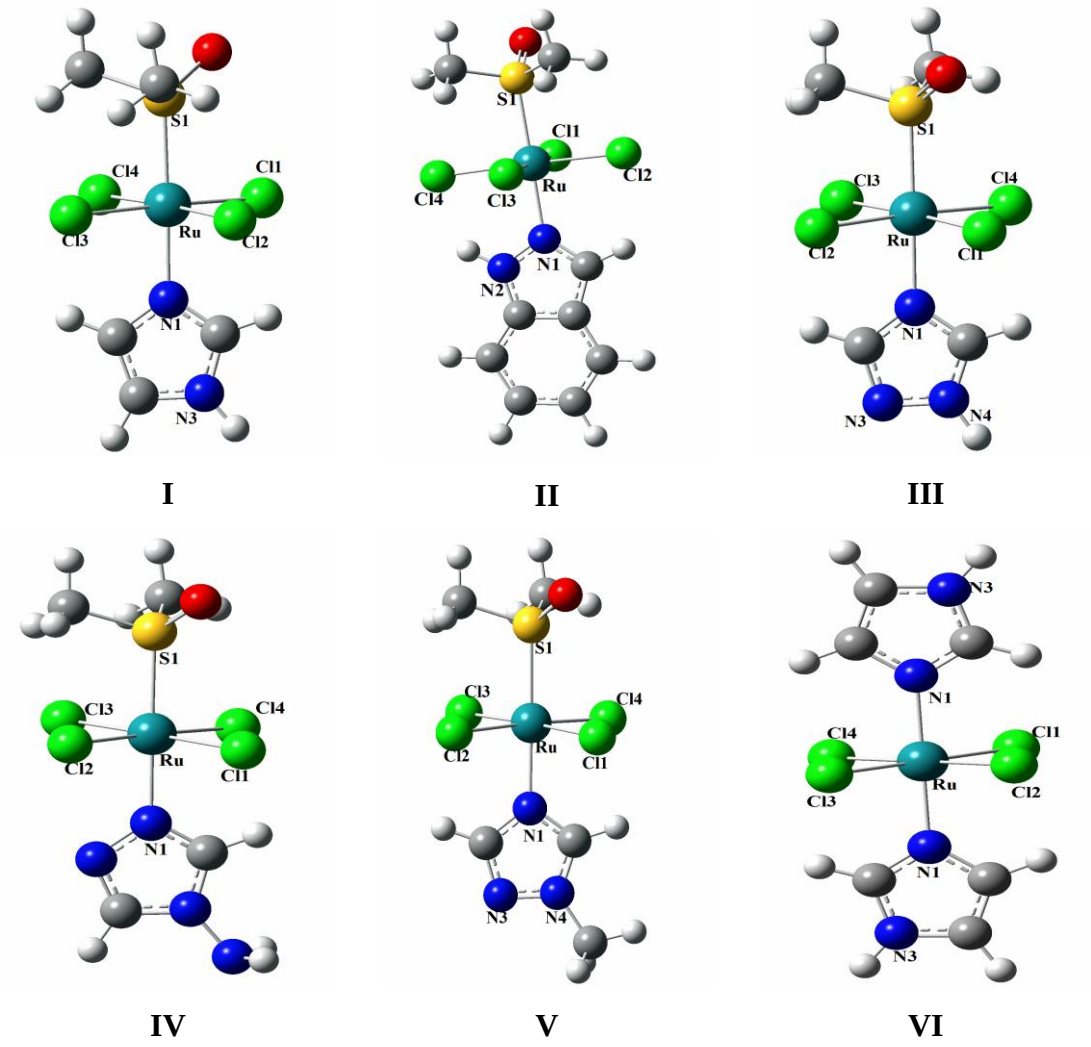

Fig. 3.1 Optimized geometries of ruthenium (III) complexes with appropriate numbering obtained from B3LYP/ (LanL2DZ+6-31G(d,p) calculation.

3.3.2 Global reactivity

The calculated chemical hardness (η), chemical potential (μ) and electrophilicity (ω) values for the ruthenium(III) complexes (in gas as well as solvent phases) are shown in Table 3.2. Maximum hardness principle states that the most stable compound has the maximum hardness value.[41] It seen from Table 3.2 that complex **VI** has the highest value of chemical hardness. Hence, Complex **VI** is least reactive in the gas phase. The least reactivity of the complex **VI** can also be predicted from the highest value of chemical potential and the lowest value of electrophilicity. On the other hand, complex **II** has the highest value of electrophilicity, (ω) and lowest value of chemical potential (μ) and hardness (η) indicate its highest reactivity. The

reactivity of ruthenium complexes changes on incorporation of solvent effect (water). The lower values of chemical hardness (Table 3.2) in solvent medium indicate the increased reactivity of all the complexes. Solvent phase calculation predicts complex **IV** as the most reactive among the ruthenium complexes in contrast to their gas phase result. The solvent molecules may coordinate with the ruthenium center by ligand exchange or may interact with the ligand coordinated to the ruthenium ion through hydrogen bond, affecting the reactivity of the metal complexes. Higher reactivity of complex **IV** agrees well with the experimental results reported by Grossl *et al.*[40] They have investigated the activity of some ruthenium(III) anticancer complexes by measuring the half-life of binding to plasma proteins *in vitro* and found higher reactivity of complex **IV**. Again, it is observed that all the complexes have higher values of electrophilicity (ω) in solvent medium than that in the gaseous medium. This variation indicates that with the inclusion of solvent effect, ruthenium complexes have exhibited higher electrophilicity values, which might be the reason behind higher cytotoxic effect of these complexes.

Table 3.2 Calculated hardness (η in eV), chemical potential (μ in eV), electrophilicity (ω in eV), local philicity (ω^+ in eV) for all complexes in gas phase and solvent phase. Local philicity value for the ruthenium atom is reported.

Complexes	Gas phase				Solvent phase			
	η	μ	ω	ω^+	η	μ	ω	ω^+
I	1.280	-1.066	0.443	0.872	1.260	-4.856	9.356	16.260
II	1.213	-1.407	0.816	1.342	1.206	-4.988	10.319	13.198
III	1.282	-1.278	0.637	1.296	1.276	-4.966	9.667	17.454
IV	1.264	-1.064	0.448	0.986	1.202	-5.106	10.850	24.031
V	1.281	-1.233	0.594	1.145	1.274	-4.978	9.727	16.759
VI	1.289	-0.439	0.075	0.066	1.207	-4.451	8.207	13.928

3.3.3 Local reactivity

Local philicity (ω_k^+ at k site) is one of the most widely used local reactivity descriptor to describe the relative reactivity of a chemical species undergoing nucleophilic attack. Ruthenium anticancer drug-DNA binding mechanism involves the

nucleophilic attack at ruthenium atom. Hence, we have calculated local philicity (ω^+) for ruthenium atom of all the complexes in gas and solvent phases and these values are presented in Table 3.2. The gas phase reactivity order of ω^+ is found to be: complex **II** > complex **III** > complex **V** > complex **IV** > complex **I** >complex **VI.** Interestingly, the solvent phase reactivity order of ω^+ are found to be different compared to their respective counterparts in the gas phase. This difference in reactivity trend may be due to the different extent of solvation for different ruthenium complexes. On the other hand, the solvent phase ω^+ values of all the complexes are found to be higher than their gas phase values (Table 3.2) which indicates that ruthenium atom of all the studied complexes are chemically softer in solvent phase than that of gas phase.

3.3.4 QSAR study

Quantitative structure-activity relationship (QSAR) experiment has been done on ruthenium(III) complexes using simple linear regression analysis based on their observed anticancer activity. For this purpose cytotoxicity (IC_{50}) values of the ruthenium complexes against a HT-29 colon carcinoma cell line have been taken from the experimental results reported by Grossl *et al*.[40] These cytotoxicity (IC_{50}) values are converted to log IC_{50}^{-1} form for practical utility in QSAR analysis. Simple linear regression analysis is performed for solvent and gas phases with different reactivity descriptors namely hardness (η), chemical potential (μ), electrophilicity (ω), local philicity (ω^+) etc. We utilize the reactivity descriptor as independent variable while, experimental cytotoxic activity ($\log IC_{50}^{-1}$) values as a dependent variable both in the gas and solvent phases. It is observed that the cytotoxic activity of the complexes cannot be predicted by hardness (η), chemical potential (μ) and electrophilicity (ω) values. However, solvent phase local philicity (ω^+) values can predict the cytotoxic activity of the complexes correctly indicating the significance of solvent model for studying biomolecules.

The modeled regression equation obtained in the solvent phase is as follows:

$$\text{Solvent phase:} \quad \log IC_{50}^{-1} = -1.886 - 0.038 \times \omega^{+} \qquad (3.1)$$

$$n=6, \quad r= 0.954 \quad r^2=0.910, \quad SE= 0.048, \quad F= 40.72, \quad p<0.05$$

Where r is the correlation coefficient, r^2 is the square of correlation coefficient, F is the overall F-statistics for the addition of each successive term, p is the value using the F statistics and SE is the root mean square error of regression. The modeled regression eq. (3.1) obtained with r^2 value 0.910 is statistically significant. A correlation plot between experimental cytotoxicity ($\log IC_{50}^{-1}$) and calculated cytotoxicity ($\log IC_{50}^{-1}$) values of ruthenium complexes in solvent phase is shown in Fig 3.2 which indicates that this reactivity parameter (ω^{+}) can successfully be used in the prediction of cytotoxicity of ruthenium complexes.

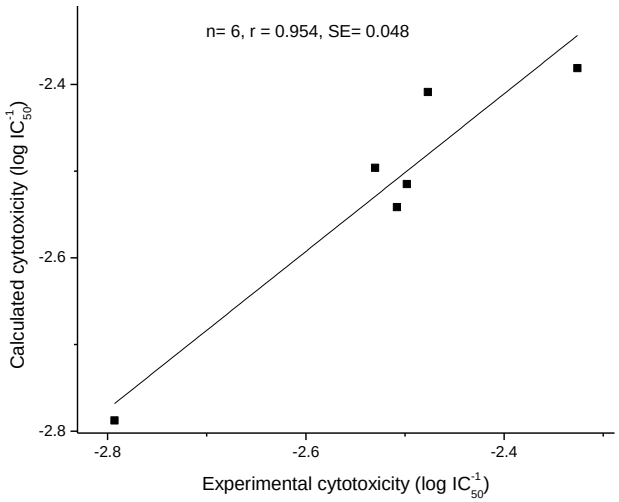

Fig. 3.2 Plot of experimental and calculated cytotoxicity ($\log IC_{50}^{-1}$) values of ruthenium complexes against HT-29 colon carcinoma cell line.

3.4 Conclusion

Systematic DFT calculations have been carried out in order to investigate the structure, stability and reactivity of some ruthenium(III) anticancer complexes in gas and solvent phases. The significant geometrical parameters of the ruthenium complexes calculated in both gas and solvent phases correlate well with available experimental results. Calculated global reactivity descriptors reveal that complex **II** is more reactive in gas phase. However, with the inclusion of solvent effect reactivity

trend of ruthenium complexes found to be different. Complex **IV** is calculated to be the more reactive in solvent phase. The generated QSAR model is very informative as they show good correlation with the experimental results. QSAR result indicates the importance of local philicity in the prediction of structure-activity relationship of ruthenium complexes.

References

1. M. A. Jakupec, M. Galanski, B. K. Keppler, *Rev. Physiol. Biochem. Pharmacol*., 2003, **146**, 1-54.
2. Z. Travnicek, M. Matikova-Malarova, R. Novotna, J. Vanco, K. Stepankova, P. Suchy, *J. Inorg. Biochem.*, 2011, **105**, 937-948.
3. M. Bouma, B. Nuijen, M. T. Jansen, G. Sava, A. Flaibani, S. Bult , J. H. Beijen, *J. Pharm. Biomed. Anal*., 2002, **30**, 1287-1296.
4. M. Brindell, I. Stawoska, J. Supel, A. Skoczowski, G. Stochel, R. van Eldik, *J. Biol. Inorg. Chem*., 2008, **13**, 909-918.
5. E. Reisner, V. B. Arion, B. K. Keppler, A. J. L. Pombeiro, *Inorg. Chim. Acta*., 2008, **361**, 1569-1583
6. M. J. Clarke, *Chem. Rev*., 2003, **236**, 209-233.
7. S. Rockwell, I. T. Dobrucki, E. Y. Kim, S. T. Marrison, V. T. Vu, *Curr. Mol. Med*., 2009, **9**, 442–458.
8. G. Sava, A. Bergamo, S. Zorzet, B. Gava, C. Casarsa, M. Cocchietto, A. Furlani, V. Scarcia, B. Serli, E. Iengo, E. Alessio, G. Mestroni, *Eur. J. Cancer*, 2002, **38**, 427-435.
9. M. A. Jakupec, E. Reisner, A. Eichinger, M. Pongratz, V. B. Arion, M. Galanski, C. G. Hartinger, B. K. Keppler, *J. Med. Chem*., 2005, **48**, 2831-2837.
10. T. Pieper, K. Borsky, B. K. Keppler, *Topics Bioinorg. Chem.*, 1999, **1**, 171-199.
11. P. Schluga, C. G. Hartinger, A. Egger, E. Reisner, M. Galanski, *Dalton Trans*., 2006, **14**, 1796-1802.
12. M. Webb, C. Walsby, *Dalton Trans.*, 2011, **40**, 1322-1331.
13. C. A. Smith, A. J. Sutherland-Smith, B. K. Keppler, F. Kratz, E. N. Baker, *J. Biol. Inorg. Chem*., 1996, **1**, 424-431.
14. A. Casini, C. Temperini, C. Gabbiani, C. T. Supuran, L. Messori, *ChemMedChem*., 2010, **3**, 1989-1994.
15. O. Mazuryk, K. Kurpiewska, K. Lewiński, G. Stochel, M. Brindell, *J. Inorg. Biochem*., 2012, **116**, 11–18.
16. A. Vergara, G. D'Errico, D. Montesarchio, G. Mangiapia, L. Paduan, A. Merlino, *Investig. New Drugs*., 2003, **21**, 401–411.

17. F. Kratz, B. Keppler, M. Hartmann, L. Messori, M. R. Berger, *Met Based Drugs*., 1996, **3**, 15–23.

18. R. G. Parr, R. G. Pearson, *J. Am. Chem. Soc.*, 1983, **105**, 7512-7516.

19. M. Berkowitz, S. K. Ghosh, R. G. Parr, *J. Am. Chem. Soc*., 1985, **107**, 6811-6814.

20. U. Sarkar, D. R. Roy, P. K. Chattaraj, R. Parthasarathi, J. Padmanabhan, V. A. Subramanian, *J. Chem. Sci*., 2005, **11**, 599-612.

21. P. P. Singh, H. K. Srivastava, F. A. Pasha, *Bioorg. Med. Chem.*, 2004, **12**, 171-177.

22. P. K. Chattaraj, S. Nath, B. Maiti, *Reactivity descriptors in computational medicinal chemistry for drug discovery.* J. Tollenaere, P. Bultinck, W. Winter, H. D. Langenaeker, M. Dekker Eds.; New York, 2003. pp. 295-322.

23. D. R. Roy, R. Parthasarathi, B. Maiti, V. Subramanian, P. K. Chattaraj, *Bioorg. Med. Chem*., 2005, **13**, 3405-3412.

24. J. Padmanabhan, R. Parthasarathi, V. Subramanian, P. K. Chattaraj, *J. Phys. Chem. A*, 2006, **110**, 9900-9907.

25. R. P. Iczkowski, J. L. Margrave, *J. Am.Chem. Soc*., 1961, **83**, 3547-3551.

26. T. A. Koopmans, *Physica*., 1993, **1**, 104-113.

27. R. G. Parr, L. V. Szentpaly, S. Liu, *J. Am. Chem. Soc*., 1999, **121**, 1922-1924.

28. R. G. Parr, W. Yang, *J. Am. Chem. Soc*., 1984, **106**, 4049-4050.

29. P. K. Chattaraj, B. Maiti, U. Sarkar, *J. Phys. Chem. A*, 2003, **107**, 4973-4975.

30. M. J. Frisch, G. W. Trucks, H. B. Schlegel, G. E. Scuseria, M. A. Robb, J. R. Cheeseman, G. Scalmani, V. Barone, B. Mennucci, G. A. Petersson, H. Nakatsuji, M. Caricato, X. Li, H. P. Hratchian, A. F. Izmaylov, J. Bloino, G. Zheng, J. L. Sonnenberg, M. Hada, M. Ehara, K. Toyota, R. Fukuda, J. Hasegawa, M. Ishida, T. Nakajima, Y. Honda, O. Kitao, H. Nakai, T. Vreven, J .A. Montgomery, J. E. Peralta, F .Ogliaro, M. Bearpark, J. J. Heyd, E. Brothers, K. N. Kudin, V. N. Staroverov, T. Keith, R. Kobayashi, J. Normand, K. Raghavachari, A. Rendell, J. C. Burant, S. S. Iyengar, J .Tomasi, M. Cossi, N. Rega, J. M. Millam, M. Klene, J. E. Knox, J. B. Cross, V. Bakken, C. Adamo, J. Jaramillo, R. Gomperts, R. E. Stratmann, O. Yazyev, A. J. Austin, R. Cammi, C. Pomelli, J. W. Ochterski, R. L. Martin, K. Morokuma, V. G.

Zakrzewski, G. A. Voth, P. Salvador, J. J. Dannenberg, S. Dapprich, A. D. Daniels, O. Farkas, J. B. Foresman, J. V. Ortiz, J. Cioslowski, D. J. Fox, Gaussian 09, Revision B.01, Gaussian Inc., Wallingford, CT, 2010.

31. A. D. Becke, *Phys. Rev. A*, 1988, **38**, 3098-3100.

32. C. Lee, W. Yang, R. G. Parr, *Phys Rev*., 1988, **37**, 785-789.

33. J. P. Perdew, K. Burke, Y. Wang, *Phys. Rev. B*, 1996, **54**, 16533-16539.

34. P. J. Hay, W. R. Wadt, *J. Chem. Phys*., 1985, **82**, 270-284.

35. P. C. Hariharan, J. A. Pople, *Chem. Phys. Lett*., 1972, **16**, 17-219.

36. J. Andzelm, C. Koelmel, A. Klamt, *J. Chem. Phys*., 1995, **103**, 9312-9320.

37. MATLAB, The Math Works, Inc., Natick, USA, 2010.

38. J. Chen, L. Chen, S. Liao, K. Zheng, L. Ji, *J. Phys. Chem. B*, 2007, **111**, 7862-7869.

39. E. Reisner, V. B. Arion, M. F. C. Guedes da silva, R. Lichtenecker, A. Eichinger, B. K. Keppler, V. Y. Kukushkin, A. J. Pombeiro, *Inorg. Chem*., 2004, **43**, 7083-7093.

40. M. Grossl, E. Reisner, C. G. Hartinger, R. Eichinger, O. Semenova, A. R. Timerbaev, M. A. Jakupec, V. B. Arion, B. K. Keppler, *J. Med. Chem*., 2007, **50**, 2185-2193.

41. R. G. Parr, P. K. Chattaraj, *J. Am. Chem. Soc*., 1991, **113**, 1854-1855.